International Journal of Nanomedicine

Dovepress
open access to scientific and medical research

Open Access Full Text Article

ORIGINAL RESEARCH

A Peptide-Functionalized Magnetic Nanoplatform-Loaded Melatonin for Targeted Amelioration of Fibrosis in Pressure Overload-Induced Cardiac Hypertrophy

This article was published in the following Dove Press journal:
International Journal of Nanomedicine

Xueli Zhao[1]
Xuanying Wang[1]
Jing Wang[1]
Jiani Yuan[1]
Juan Zhang[1]
Xiaoli Zhu[1]
Changhui Lei[1]
Qianli Yang[1]
Bo Wang[1]
Feng Cao[2]
Liwen Liu[1]

[1]Department of Ultrasound of Xijing Hospital, Xijing Hypertrophic Cardiomyopathy Center, Fourth Military Medical University, Xi'an 710032, People's Republic of China; [2]Department of Cardiology, Chinese PLA General Hospital, Beijing 100700, People's Republic of China

Introduction: Currently, the unsatisfactory treatment of cardiac hypertrophy is due to the unbridled myocardial fibrosis. Melatonin has been demonstrated to ameliorate cardiac hypertrophy and its accompanied fibrosis in previous studies. But it is not clinically appealing due to its short-lasting time against the hostile microenvironment when administered orally.

Methods: Herein, to address this, poly (lactide) polycarboxybetaine (PLGA-COOH) accompanied by cardiac homing peptide (CHP) and superparamagnetic iron oxide nanoparticles (SPIONs) were used to establish a novel drug delivery and transportation strategy for melatonin via a facile two-step emulsion method. This study characterized these nanoparticles (CHP-mel@SPIONs) and tested their delivery to the hypertrophied heart and their effect on myocardial hypertrophy and fibrosis in an animal model of pressure overload-induced cardiac hypertrophy.

Results: The engineered magnetic nanoparticles of CHP-mel@SPIONs were spherical (diameter = 221 ± 13 nm) and had a negative zeta potential of −19.18 ± 3.27 mV. The CHP-mel@SPIONs displayed excellent drug encapsulation capacities of SPIONs (75.27 ± 3.1%) and melatonin (77.69 ± 6.04%) separately, and their magnetic properties were characterized by constructing magnetic hysteresis curves and exhibited no remnant magnetization or coercivity. The animal experiments showed that compared with mel@SPIONs, CHP-mel @SPIONs accumulated more in the heart, especially in the presence of an external magnetic field, with in vivo echocardiography and RT-PCR and histological assessments confirming the amelioration of the myocardial hypertrophy and fibrosis with low drug doses.

Conclusion: This simple biocompatible dual-targeting nanoagent may be a potential candidate for the guided clinical therapy of heart disease.

Keywords: magnetic targeting, cardiac homing peptide, cardiac hypertrophy, melatonin, myocardial fibrosis

Introduction

Cardiac hypertrophy is a progressive pathological compensatory reaction to chronic pressure overload.[1,2] Most cardiac hypertrophy patients exhibit excessive myocardial fibrosis,[3] which not only interferes with the systolic and diastolic functions, but is also associated with worse clinical outcomes such as malignant ventricular arrhythmia, heart failure (HF) and sudden death.[4–6] It is therefore important to address excessive myocardial fibrosis in cardiac hypertrophy. But current clinical

Correspondence: Liwen Liu
Email liuliwen@fmmu.edu.cn

treatments aimed only at alleviating the symptoms without reducing the fibrosis itself. Hence, there is a great need for a treatment that reverses myocardial fibrosis, but this remains a big challenge.

Melatonin (N-acetyl-5-methoxytryptamine, Mel), a ubiquitous and versatile molecule secreted by the pineal gland in a rhythmic manner, is highly beneficial for functioning living organs and tissues.[7,8] In particular, it plays a cardiac–protective role in conditions such as ischaemia–reperfusion injury, atherosclerosis, diabetic cardiomyopathy, pathological hypertrophy and heart failure.[9–14] More recently, one of the underlying mechanisms of melatonin's cardiac-protective role has shed light on its anti-fibrosis effects in the heart.[15–17] Melatonin can protect diabetic myocardium from diastolic chamber stiffness and diastolic dysfunction.[18] Melatonin can attenuate cardiac fibrosis by inhibiting the TGFb1–Smad3 signaling pathway.[19] Furthermore, pathological fibrosis results in the deposition of extracellular matrix (ECM), and melatonin contributes to its reduction.[20,21] Thus, there is substantial evidence that melatonin could play a potentially important role in the treatment and prevention of fibrosis existing in cardiac hypertrophy. However, melatonin is conventionally administered orally, which involves several drawbacks that affect its efficiency as a treatment for fibrosis, including oral fast-release, low bioavailability and tolerance insurgence. There is, therefore, a need for an efficient new strategy for targeted delivery of melatonin.[22–24]

Superparamagnetic iron oxide nanoparticles (SPIONs) have emerged as a promising targeted drug delivery platform because of their unique magnetic property, which is ideal for in vivo use.[25,26] SPIONs can be highly magnetized, allowing associated drug molecules to be dragged to the target site in the body under the influence of an external magnetic field. There has been increasing interest in SPIONs–drug associates, especially with regard to their potential role in targeted therapy. However, the major drawback of the SPION–drug system is its lack of accuracy in targeting intended tissues, which has resulted in unsatisfactory therapeutic effects and the risk of normal tissues being damaged in the magnetic field.

Recently, a cardiac homing peptide (CHP, comprising the peptide motif CSTSMLKAC) has been developed to enhance the specificity and efficiency of directly targeting nanoparticles to hypertrophied myocardium.[27–29] This is achieved through its high sensitivity to ischaemic cardiac tissue, which can result from continuous cardiac hypertrophy.[30]

In this study, we described and tested a dual-targeting nanoplatform that used CHP and SPIONs for the targeted delivery of melatonin to hypertrophied heart tissue under an external magnetic field. We hypothesized that this nanoplatform, CHP-mel@SPIONs, would provide accurate and effective treatment for pressure overload-induced cardiac hypertrophy and its associated myocardial fibrosis. If so, then this nanoplatform may have a strong potential for clinical application.

Experimental

Materials

Oleic acid-coated SPIONs (d = 10 nm, 5 mg/mL) were purchased from Xi'an ruixi Biological Technology Co., Ltd. (China). CHP and fluorescein isothiocyanate (FITC)-CHP were purchased from GL Biochem Ltd. (Shanghai, China). PLGA-COOH (50:50, MW ¼ 20,000) was obtained from Jinan Daigang Biomaterial Co., Ltd. (China). Melatonin was purchased from Sigma-Aldrich (St. Louis, MO, USA). MES (2-(N-morpholino)ethane sulfonic acid) hydrate, EDC (1-ethyl-3-(3-dimethylaminopropyl)-carbodiimide hydrochloride), NHS (*N*-hydroxysuccinimide) were obtained from Sigma-Aldrich Chemical Co. (St. Louis, MO, USA). The fluorescent dyes DAPI (4′,6-diamidino-2-phenylindole), DiI (1,1′-dioctadecyl-3,3,3′,3′ tetramethylindocarbocyanine perchlorate) and DiR (1,1′-dioctadecyl-3,3,3′,3′-tetramethylindotricarbocyanine iodide) were also obtained from Sigma-Aldrich Chemical Co. Deionized water was used in the preparations.

Preparation of CHP-mel@SPIONs

The magnetic and CHP-based dual-targeting nanoparticles, CHP-mel@SPIONs, were prepared as previously described.[31] Briefly, 100 mg PLGA-COOH, 200 μL SPIONs and 20 mg melatonin were completely dissolved in 2 mL dichloromethane (CH_2Cl_2). When preparing fluorescent nanoprobes, a few drops of DiI fluorescent dye were also added. The solution slowly dropped from an injection syringe into 10 mL 4% PVA solution, which was emulsified using an ultrasonic probe (Ultrasonic Cell Crusher JN-900D, Ningbo, China) at 450 W for 10 min (with a vibration on/off cycle of 1.2 s/0.8 s to prevent overheating), followed by organic phase evaporation. The solution was then centrifuged at 13,000 rpm for 10 min. Finally, the precipitate was washed three times and adjusted to the final concentration using phosphate-buffered saline (PBS).

Targeted CHP-mel@SPIONs were prepared based on a method used for carbodiimides. First, the prepared mel@SPIONs were dispersed in 10 mL MES buffer (0.1 mol/L, PH = 5.5) together with 24 mg EDC and 12 mg NHS (a mixed coupling activator) for oscillation and incubated for 1 h. Residual EDC and NHS were extracted using MES buffer (0.1 mol/L, pH = 5.5) after being centrifuged three times for 10 min at 13,000 rpm. The precipitate was then redissolved in MES buffer (0.1 mol/L, pH = 8.0), and 1 mL CHP peptide solution (1 mg/mL) was dropped into the above solution followed by overnight incubation with continuous shaking. Afterward, after three consecutive centrifugations to remove unbonded CHP peptide, the final CHP-mel@SPIONs were harvested and stored at 4°C.

Characterization of CHP/mel@SPIONs

The size distribution, polydispersity index and surface zeta potential of the prepared nanoparticles were determined through dynamic light scattering at 25°C using a laser particle size analyzer (DelsaNano C Particle Analyzer; USA) after equilibrating for 30 s. For a better understanding of the morphology of the prepared nanoprobes, the nanoparticles were carefully dropped onto a copper grid, negatively stained and observed by transmission electron microscopy (JEM-2100 Electron Microscope; Japan). The nanoparticle surface was examined using atomic force microscopy (Agilent 5500 Scanning Probe Microscope; USA) performed at 25°C on a silicon slice with a general-purpose tapping tip (tip height, 10–15 µm; cantilever thickness, 7.0 ± 1.0 µm; cantilever width, 38 ± 7.5 µm; cantilever length, 225 ± 10 µm; resonance frequency, 146–236 kHz; force constant, 21–98 Nm^{-1}; NANOSENSOR, USA). The atomic force microscopy images were then analyzed using Pico Image Elements 7.2 software (USA). The conjugation efficiency for the attachment of CHP onto the shells of the nanoparticles was determined by incubating mel@SPIONs with FITC-labelled CHP peptide overnight. The labeled nanoparticles were then observed under a Nikon A1 confocal laser scanning microscope (Nikon, Japan). Magnetic hysteresis curves were obtained with a superconducting quantum interference device (Quantum Design, USA) under a magnetic field of 15 kOe at 300 K.

Encapsulation Efficiency of CHP-mel@SPIONs for SPIONs and Melatonin

The encapsulation efficiency of CHP-mel@SPIONs for SPIONs was determined by inductively coupled plasma mass spectrometry, as follows. The suitable standard dilutions of Fe (GBW(E)080123; National Institute of Metrology, China) were prepared in 20% nitric acid to obtain a standard curve for the range 1–100 ng/mL. CHP-mel@SPIONs samples were digested in 5 mL of nitric acid and incubated overnight at 4°C. The resulting solution was diluted to achieve concentrations within the calibration range. The Fe content was measured by inductively coupled plasma mass spectrometry (NexION 350D; PerkinElmer, USA). The encapsulation efficiency of CHP-mel@SPIONs or CHP-mel for melatonin was analyzed using a UV-visible absorption spectrometer (HALO DB-20R; Dynamica, Australia) at a wavelength of 278 nm according to the standard curve.

Drug Release Profile in vitro

The release profile for melatonin from CHP-mel@SPIONs in vitro was characterized by a dialysis method. Briefly, 2 mL of CHP-mel@SPION solution (containing 2 mg/mL melatonin) was placed into a dialysis membrane (MW 3500 Da) and then submerged in 30 mL of sustained-released PBS medium (containing 0.1% Tween-80) at PH 7.4, and this was then incubated in a vibrating water bath at 37°C (to simulate body temperature). At fixed intervals, 2 mL of dialysate was extracted, and the solution was replenished with an equal volume. The melatonin concentrations at different time points were detected by UV-visible absorption spectrometry. The cumulative release of melatonin from CHP-mel@SPIONs was calculated and plotted as the release ratio against time.

Animal Model of Cardiac Hypertrophy and Treatments

All animals received care in compliance with the Guidelines for the Care and Use of Laboratory Animals of the animal ethics committee of Fourth Military Medical University (Licence number: SYXK 2019–001). As described previously,[32] Sprague–Dawley rats (200–250 g), housed under optimum conditions, were anesthetized and subjected to transverse aortic constriction surgery (TAC) to induce cardiac hypertrophy or a sham surgical procedure without aortic ligation. The groups were set as sham surgery group (sham), TAC rats treated with saline group (TAC), TAC rats treated with mel@SPIONs (mel@SPIONs), TAC rats treated with CHP/mel@SPIONs (CHP/mel@SPIONs) and TAC rats treated with CHP/mel@SPIONs exposed to an external magnetic field (CHP/mel@SPIONs + M). The external magnetic field was achieved using a 0.6-T neodymium permanent magnet positioned outside the heart for 2 h after injection of the nanodroplets. The treatments began after a recovery period of 1 week and were administered once every 3 days for 8 consecutive weeks. Table 1 lists the study design of the animal experiment.

At the endpoint of the experiments, the rats were sacrificed. The wet weights of the heart and left ventricle were determined and normalized to the animal's body weight. The left ventricular tissue samples were immersed in paraformaldehyde (4%), embedded in paraffin and sectioned serially (5–6 µm sections). The slides were stained with hematoxylin and eosin (HE) or Masson trichrome for evaluation of cross-sectional areas of cardiomyocytes and collagen deposition, respectively. The remaining portions were snap-frozen in liquid nitrogen for subsequent real-time reverse transcription polymerase chain reaction (RT-PCR) analysis.

Assessment of CHP-mel@SPIONs Targeting in vivo

To assess the targeting ability of CHP-mel@SPIONs, rats were anesthetized with intraperitoneal injections of 1% sodium pentobarbital (40 mg/kg). Once they were motionless, 1 mL of DiI-labelled mel@SPIONs or CHP-mel@SPIONs was injected via the tail vein. At 48 h after injection, rats were sacrificed, and their hearts and other major organs were harvested and frozen. According to the standard protocol described in Cryosectioning Tissues,[33] 4–5 µm cryosections were continuously cut at a temperature of −20°C. After fixation for 15 min in 4% paraformaldehyde, the cryosections were stained with DAPI dye for 10 min in the dark to visualize the cell nuclei. After washing 3 times with PBS, the fluorescence distributions on the sealed slides were photographed with a confocal laser scanning microscope.

To further confirm the accumulation of the nanoparticles, cross-sections from the treated hearts were stained with Prussian blue to detect the presence of iron. The organs of different formulations, including the heart, liver, spleen, lung and kidney, were harvested for Prussian blue staining after 48 h treatment.

Iron Concentration Assay in vivo

Rats were sacrificed 48 h after intravenous administration, the concentrations of iron of the tissues including heart, liver, spleen, lung and kidney were evaluated using Iron Assay Kit (Sigma-Aldrich). The absorbance (OD) of the samples was tested at 593 nm.

Cardiac Function Analysis

Cardiac function in response to cardiac hypertrophy and nanoparticle therapy was evaluated by echocardiography. The anesthetized rats were placed on the stage of a vevo 2100 Imaging System (Visual Sonics imaging system, Canada), and serial B-mode and M-mode echocardiography were acquired along the short axis of the left ventricle at the level of the papillary muscles. The following parameters of left ventricular contractile function and thickness were measured on M-mode echocardiography as reported previously,[34,35] including interventricular septum end-diastolic thickness (IVSd), interventricular septal end-systole thickness (IVSs), posterior end-diastolic wall thickness (LVPWd), posterior end-systole wall thickness (LVPWs), left ventricular ejection fraction (LVEF) and left ventricular fractional shortening (LVFS).

Measurement of Hydroxyproline

To assess collagen levels in the hearts of the five treatment groups, hydroxyproline concentrations were measured in samples from left ventricles by stepwise treatment with various buffers according to the instructions of a hydroxyproline kit (Nanjing Jiancheng Bioengineering Institute, Nanjing, China) as described previously.[36] The hydroxyproline concentrations were then estimated spectrophotometrically using a SpectraMax M5 microplate reader (Molecular Devices, CA, USA) at 550 nm.

Table 1 A Diagram for Study Design of Animal Experiment

Groups	Sham	TAC	mel@SPIONs	CHP/mel@SPIONs	CHP/mel@SPIONs + M
Numbers	10	10	10	10	9
Treatment	Administered once every 3 days for 8 consecutive weeks, CHP/mel@SPIONs + M group received a external magnetic field outside the heart for 2 h after injection of the nanodroplets. Rats were administered with the nanoparticles once every 3 days for 8 weeks.				

HE and Masson's Trichrome Staining

After euthanizing the animals, their hearts were perfused with 60 mL of cold saline and harvested. A microtome was used to cut 4–5 µm thick transversal sections from formalin-fixed left ventricular tissues. These were stained with HE and Masson's Trichrome for histopathology and collagen deposition assessments, following standard procedures. The quantitative assessments of the cross-sectional area of myocyte and the percentage of myocardial fibrosis area were performed separately using Image J (NIH) and Image-Pro Plus 6.0 (USA) software.

Real-Time Quantitative Polymerase Chain Reaction (RT-PCR)

Total RNA was extracted from flash-frozen myocardial tissues using TRIzol (Invitrogen, USA). RNA purity and concentration were assessed by determining the A260/A280 ratio with a spectrophotometer (PTC-220 Peltier DYAD; MJ Research Inc., USA). cDNA was synthesized using PrimeScript™ RT Master Mix (Takara Bio, Japan) and then amplified by specific TB Green™ Premix Ex Taq™ II (Tli RNaseH Plus) (Takara Bio) with a CFX96 real-time PCR system-C1000 thermal cycler (Bio-Rad Laboratories, Hercules, CA, USA). All reactions were performed in a final volume of 25 µL, following the manufacturer's instructions. The expression levels of target genes were presented as Ct values and shown as $2^{-\Delta\Delta Ct}$. GAPDH was used as an internal reference. Table 2 lists the primer sequences used for the RT-PCR.

Statistical Analysis

The figures present data as mean values with the error bar indicating the standard deviation. One-way analysis of variance was used for the statistical evaluations. The statistical analysis was performed using GraphPad Prism (GraphPad Software, Inc., La Jolla, CA). P-values <0.05 were considered to indicate statistical significance.

Results and Discussion

Preparation and Characterization of Magnetic Nanoparticles (CHP/mel@SPIONs)

In this study, we synthesized targeted magnetic nanoparticles, CHP-mel@SPIONs, to assess our strategy for enhanced targeted delivery of melatonin to the heart. The nanoparticles were synthesized via a two-step emulsion method that encapsulated melatonin, SPIONs and CHP in the shell simultaneously. The structural characteristic of the nanoparticles was first confirmed by atomic force microscopy. This showed them to be spherical, with homogeneous size and height (Figure 1A–C). The phase image of atomic force microscopy can be used to distinguish the different surface features and is useful for the compositional mapping of surfaces and interfaces of nanoparticles.[37] Figure 1C showed a full view of a three-dimensional reconstruction of a CHP-mel@SPIONs. Transmission electron microscopy was then used to investigate the internal structure of CHP-mel@SPIONs. This suggested that SPIONs were homogenously encapsulated in the CHP-mel@SPIONs (Figure 1D). The size, estimated from dynamic light scattering, was around 221 ± 13 nm (Figure 1F), which was consistent with the TEM findings, and the polydispersity index was <0.1, confirming the homogeneity of all the preparations. The zeta potential of mel@SPIONs and CHP-mel@SPIONs was −31.34 ± 2.61 mV and −19.18 ± 3.27 mV separately (Figure 1E). A negative surface charge can prolong nanoparticle blood circulation and prevent cytotoxicity caused by the proton-sponge effect.[38] The CHP-mel@SPIONs displayed excellent drug encapsulation capacities of SPIONs (75.27 ± 3.91%) and melatonin (77.69 ± 6.04%) separately. And

Table 2 Sequences of Primers for RT-PCR

Gene	Forward Primer (5′-3′)	Reverse Primer (5′-3′)
GAPDH	CAAGTTCAACGGCACAGTCAA	CGCCAGTAGACTCCACGACA
ANP	TGAGCCGAGACAGCAAACA	CAAAAGGCCAGGAAGAGGA
β-MHC	GGCTGGCTACAGAAGAACAAG	CACGGTCTGAAAGGATGAGC
Collagen1	AACTTTGCTTCCCAGATGTCC	CATCATCTCCGTTCTTGCCA
Collagen3	CCTGGTGGGAAAGGTGAAAT	CCCTTTGCTCCATTCTTGC
TGF-β1	GACCGCAACAACGCAATCT	TACCAAGGTAACGCCAGGAAT
MMP-9	TCTTCAAGGACGGTCGGTAT	AAGGCTGAGTTCAACTTTGCA
Smad-3	CCTGGCTACCTGAGTGAAGATG	TGTAGGTCCAAGTTATTGTGTGCT

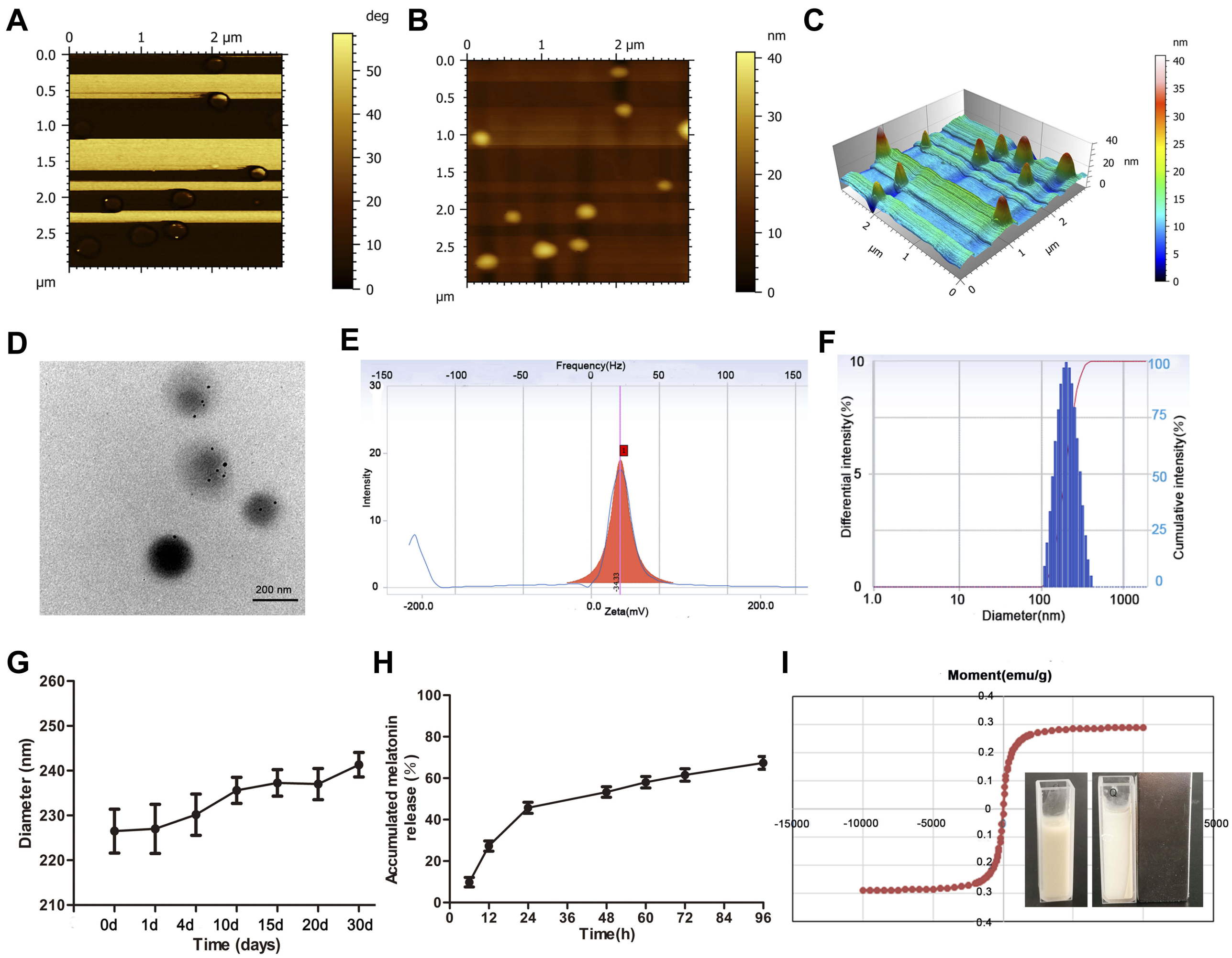

Figure 1 Characterizations of CHP/mel@SPIONs. (**A–C**) AFM measurements of the prepared CHP/mel@SPIONs ((**A**) phase image; (**B**) height image; (**C**) 3D image). (**D**) TEM image of CHP/mel@SPIONs. (**E, F**) Size distribution and Zeta potential of CHP/mel@SPIONs. (**G**) Size changes of CHP/mel@SPIONs at 4°C after long-term storage (n = 3). (**H**) In vitro melatonin releasing curves of CHP/mel@SPIONs, datas are expressed as the percentage of total melatonin. (**I**) Magnetization curves of CHP/mel@SPIONs, the inserted picture shows the magnetic separation for CHP/mel@SPIONs.

the encapsulation efficiency of melatonin in CHP-mel was 85.10 ± 5.28%. Furthermore, after 30 days of storage at 4°C, there was no remarkable change in the diameters of CHP-mel@SPIONs (Figure 1G), indicating their excellent stability during storage.

The in vitro drug release profile of CHP-mel@SPIONs was shown in Figure 1H. The profile showed that melatonin was released from nanoparticles in a typical biphasic pattern, with approximately 50% released in the initial 24 h before reaching a plateau and the releasing speed of melatonin in the later phase is relatively slow. The plateau percentages of melatonin release observed over a period of 96 h were nearly 70%, this indicated that CHP-mel @SPIONs released melatonin in a controlled manner.

The magnetic properties of targeted drug carriers are of great importance. The magnetic properties of CHP-mel @SPIONs were assessed from magnetic hysteresis curves. Figure 1I showed that the magnetic hysteresis curves exhibited no remnant magnetization or coercivity at room temperature, and the superparamagnetic characteristics were retained in the final nanoparticles. The magnetic response of CHP-mel@SPIONs was also confirmed. A magnet induced the rapid accumulation of the nanoparticles onto the wall of the cuvette, indicating their sensitivity to a magnetic field. Thus, CHP-mel@SPIONs are potentially useful for magnet-assisted targeting, which is a promising technique for enhancing the local accumulation of drug-encapsulated vehicles.

To improve the ability of the nanoparticles to target the hypertrophic heart, a myocardium-targeted peptide, CHP, was conjugated to the surface of mel@SPIONs. The CHP conjugation was determined by examining the extent of connections between FITC-labelled CHP and DiI-labelled mel@SPIONs nanodroplets. As shown by the merged orange images in Figure 2, there was a perfect connection between the mel@SPIONs nanoprobes (red) and CHP peptides (green). These results meant that CHP-mel@SPIONs had the potential to target the ischemic cardiomyocyte. In this study, we choose a bifunctional or mediator linker (EDC/NHS) to connect the CHP to the surface of mel@SPIONs, for the following reasons: 1) EDC/NHS linker does not induce any cytotoxicity in the biological systems; 2) Water solubility of waste products allows their easy washing at the end of the process; 3) Above all, NHS/EDC linker contributed to covalent attachment which showed a high controllability for immobilization of biomolecules onto the surface and provided sufficient stability of surface-active agent.[39,40]

Biodistribution and Delivery Efficiency of Modified CHP/mel@SPIONs

To assess the targeting ability of CHP-mel@SPIONs in vivo, TAC rats were injected systematically with DiI-labelled nanoparticles with or without an external magnetic field. At 48 h postinjection, the rats were sacrificed and the major organs were collected for frozen sections, with images captured using a confocal laser scanning microscope. More prominent and wide-ranging DiI-labelled nanoparticles (seen as red dots in Figure 3A) were observed in the cardiac cryosections in the group treated with CHP-mel@SPIONs than in those treated with mel@SPIONs, confirming that CHP targeting resulted in the CHP-mel@SPIONs reaching the heart area. In the group of CHP-mel@SPIONs + M, a greater number of DiI-labelled nanoparticles were observed in the heart, this could be explained by the magnetic nanoparticles being attracted by the presence of the magnet. When the other organs were assessed, the liver showed a decreased signal of nanoparticles when compared with that of mel@SPIONs. This indicated that CHP conjugation increased on-target delivery and decreased off-target delivery when CHP-mel@SPIONs were administered systemically. Although the exact mechanism by which CHP interacts with the myocardium is unknown, its conjugation to the mel@SPIONs amplified the accumulation of the nanoparticles in the heart. The half-life of melatonin administered either orally or intravenously is only approximately 45 min, which is too short to exert long-lasting effects.[22] However, this specific nanoparticle drug delivery system resulted in a controlled release and a decreased decomposition rate of melatonin, which ultimately prolongs its time of effect.

To further confirm the accumulation of the nanoparticles in the heart, cross-sections from the treated hearts were stained with Prussian blue. Figure 3B depicts that there was extremely little blue staining (black arrows) in the animals treated with mel@SPIONs and no staining in the saline group. There was more blue staining in the group treated with CHP-mel@SPIONs, with the highest level observed in the TAC rats treated with CHP-mel@SPIONs with a magnet. These results confirmed the best targeting ability of CHP-mel@SPIONs with a magnetic field again. The concentration of iron was assayed 24 h after intravenous administration of CHP-mel@SPIONs formulation (Figure 3C). The highest iron level was observed in the heart of the animals treated with CHP-mel@SPIONs + M. These findings were consistent with the fluorescent imaging results and indicated that long circulation and dual-targeting contributed to the improved accumulation of CHP-mel@SPIONs in the heart.

Cardiac Function in vivo

To investigate whether CHP-mel@SPIONs combined with an external magnetic field conferred protection

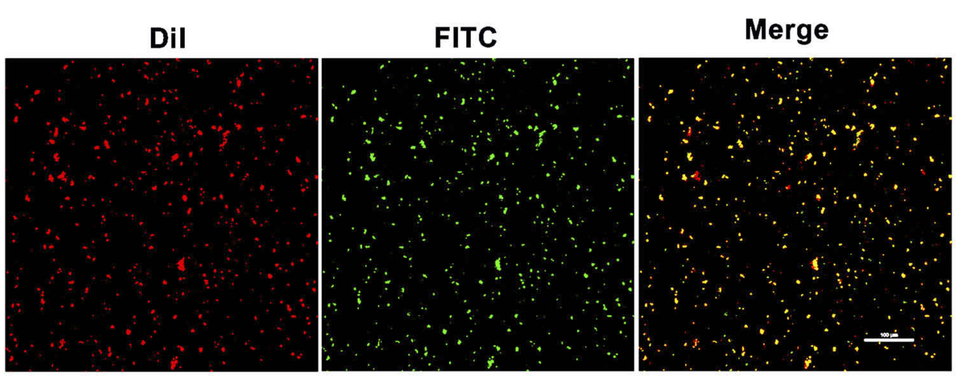

Figure 2 CLSM image results showed a preferential connection between FITC-labelled CHP peptide and DiI-labelled mel@SPIONs nanoparticles.

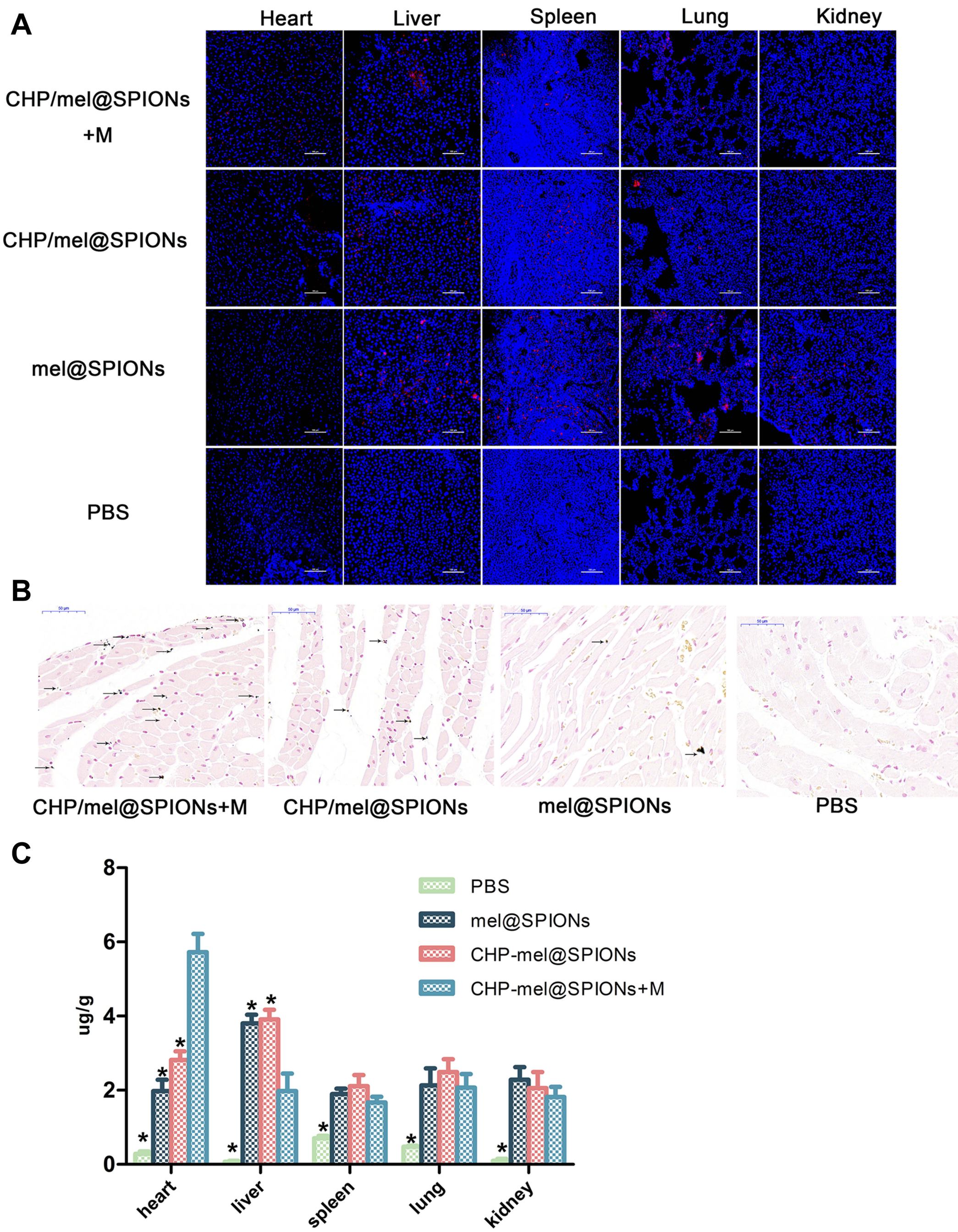

Figure 3 (**A**) CLSM analysis of cardiac sections for the experimental groups and substantial localization in other tissues such as kidney, liver, spleen and lungs from rats injected CHP/mel@SPIONs nanodroplets (magnification = 200×). (**B**) Prussian blue staining of the heart of different groups after TAC surgery (magnification = 400×). Black arrows point to blue-stained iron. (**C**) Iron biodistribution in vivo. The concentration of iron in organs after 48 h. *P < 0.05 vs CHP/mel@SPIONs+M.

against TAC-induced cardiac hypertrophy in rats, the overall morphology of the heart was assessed in vivo with echocardiography and ex vivo by measuring the weights of the total heart and left ventricle, normalized to the body weight (HW/BW and LW/BW, respectively). The animals that underwent TAC surgery exhibited marked increases in key hypertrophic parameters that indicated cardiac hypertrophy (HW/BW, LW/BW, LVPWs, LVPWd, IVSd and IVSs (Figure 4A–G). All three groups treated with melatonin nanoparticles showed considerably decreased HW/BW, LW/BW, LVPWs, LVPWd, IVSd and IVSs compared with the untreated TAC rats, indicating that melatonin has the ability to attenuate cardiac hypertrophy.

The animals treated with CHP-mel@SPIONs with an external magnetic field exhibited the greatest therapeutic effect on the hypertrophic heart reflected by all of the above six parameters than the other melatonin treatment groups, indicating clear restoration of cardiac function, perhaps due to the increased accumulation of CHP-mel@SPIONs through dual-targeting approach. LVEF and LVFS determined using echocardiography showed no obvious difference among the five groups (Figure 4H–I), indicating that left ventricular function remained compensated in the groups that underwent TAC surgery.

The two hallmarks of cardiac remodeling caused by pressure overload are cardiac hypertrophy and cardiac fibrosis.[41] To determine whether melatonin exerted a therapeutic effect on these two conditions, histological analyses using HE and Masson's staining to assess myocyte cross-section area (CSA) and cardiac collagen volume fraction (CVF) were performed using paraffin-embedded cardiac tissues. After 8 weeks of pressure overload following TAC surgery, the amounts of fibrosis and myocyte CSA increased considerably. After treatment, CSA and CVF showed a pronounced decrease in all three treatment groups compared with those in the TAC group. Furthermore, CSA and CVF were significantly lower in the CHP-mel@SPIONs + M group than in other treatment groups (Figure 5A–D).

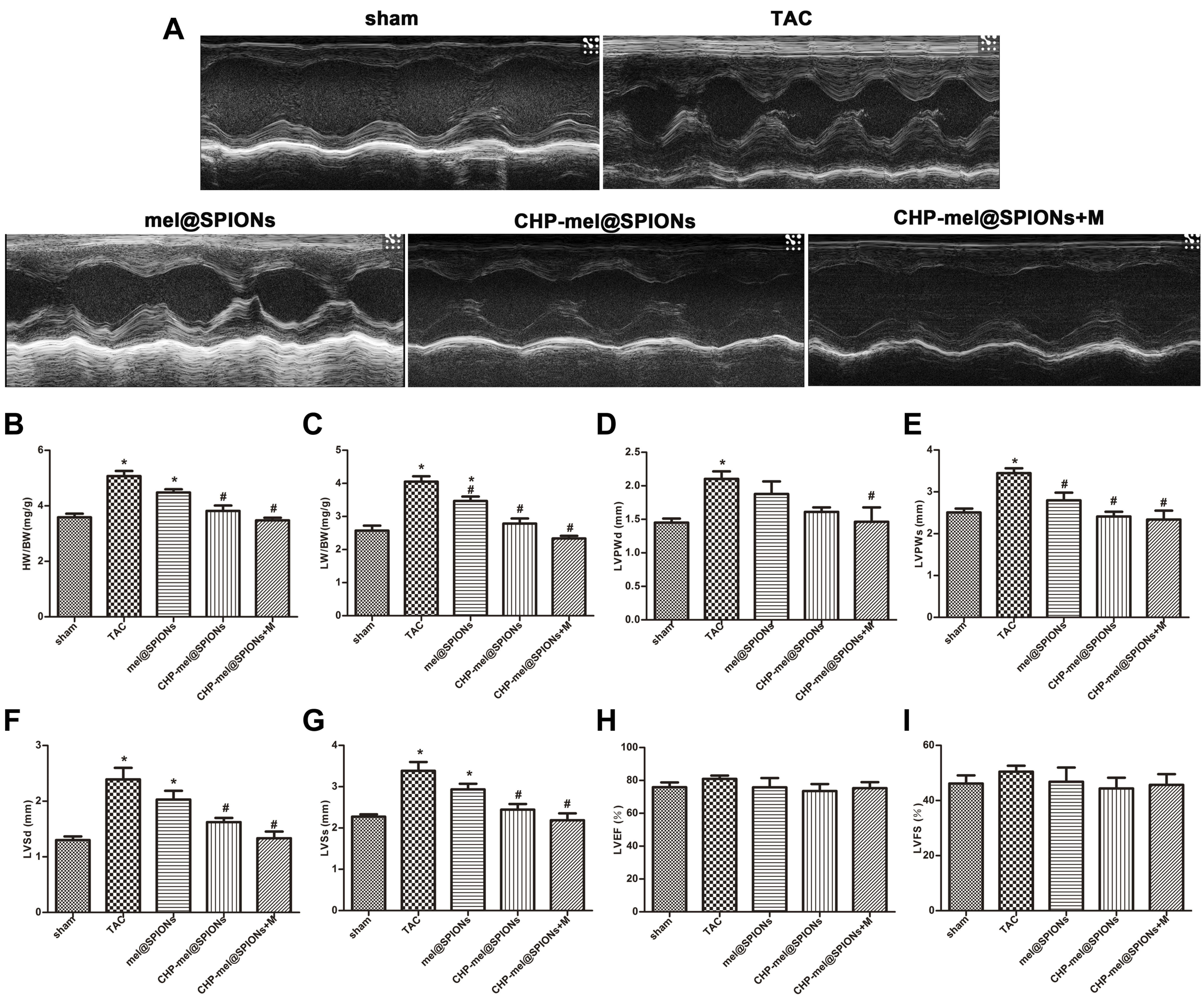

Figure 4 Effects of 8-week treatment on cardiac contractile function and wall thickness after TAC surgery. (**A**) Representative M-mode echocardiographic images. (**B, C**) The ratio of heart weight (HW) and left ventricle weight (LW) to body weight (BW). (**D**) LVPWd. (**E**) LVPWs. (**F**) IVSd. (**G**) IVSs. (**H**) LVEF. (**I**) LVFS. *P< 0.05 vs sham group; #P< 0.05 vs TAC group.

Abbreviations: LVPWd, left ventricular posterior wall thickness at end-diastole; LVPWs, left ventricular posterior wall thickness at end-systole; IVSd, interventricular septal thickness in diastole; IVSs, interventricular septal thickness in systole; LVEF, left ventricular ejection fraction; LVFS, left ventricular fractional shortening; determined by echocardiography.

To further gain insight into the effect of melatonin on the cardiac fibrosis induced by pressure overload, we measured the hydroxyproline concentration in heart tissues. As displayed in Figure 5E, the hydroxyproline concentration was increased significantly in the rat heart after TAC surgery but showed a remarkable reversal in the group treated with CHP-mel@SPIONs and an external magnetic field ($P < 0.05$). These experiments indicate that melatonin nanoparticles have better anti-fibrotic effects against TAC model.

RT-PCR analysis clearly showed that treatment with CHP-mel@SPIONs +M resulted in significant regression of cardiac hypertrophy and myocardial fibrosis, as evidenced by reduced expression of hypertrophy-related genes and myocardial fibrosis markers (Figure 6A–F). The gene expression levels of ANP and β-MHC in all three melatonin-treated groups were downregulated when compared with those in the TAC group. Fibrosis markers were markedly elevated in animals that underwent TAC surgery compared with the sham group, as shown by

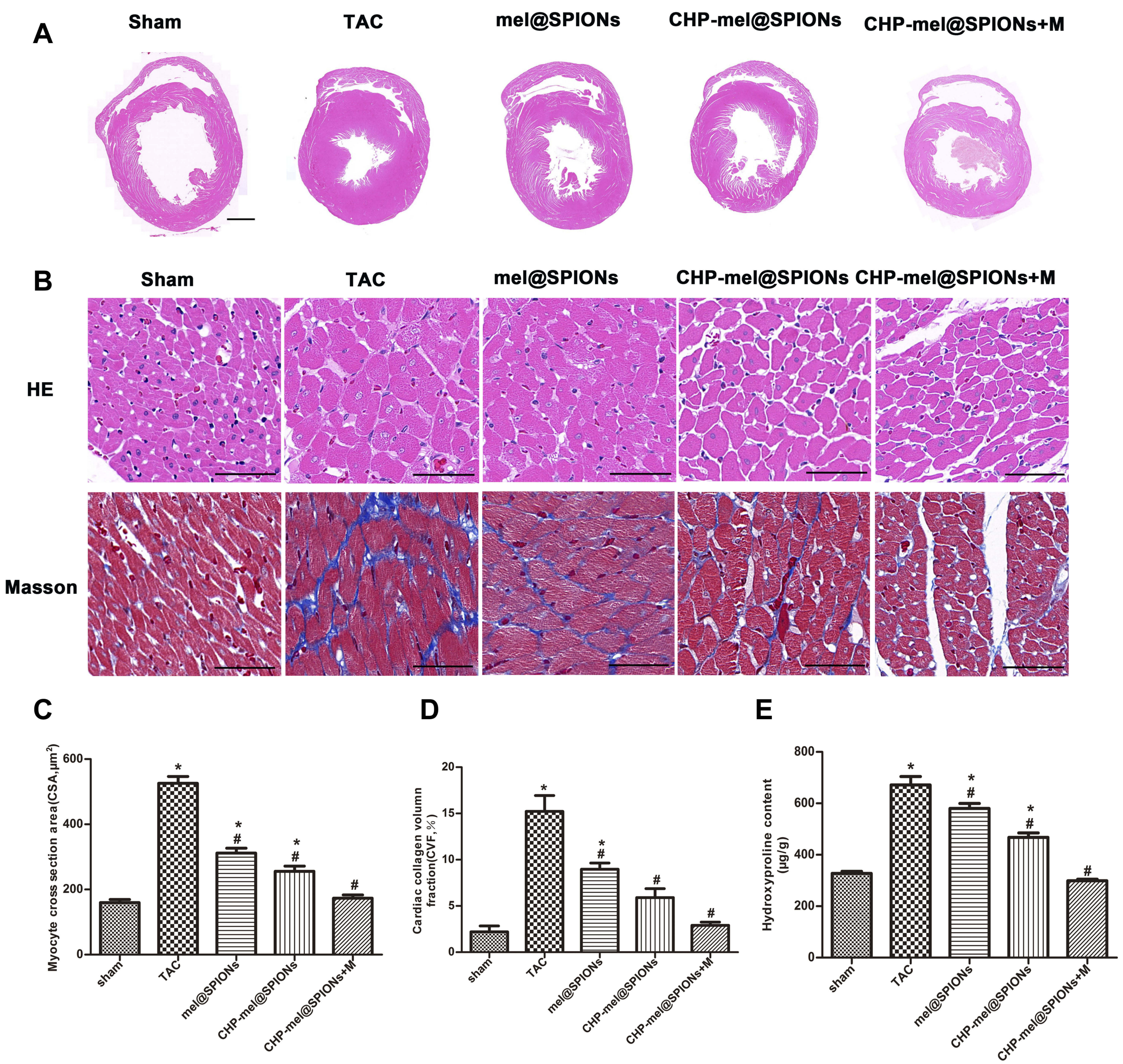

Figure 5 Regression of cardiac hypertrophy and myocardial fibrosis in experimental rats. (**A**) Representative images of HE staining of heart sections (magnification = 0.5×). (**B, C**) Representative HE staining and Masson staining images of left ventricular tissue sections (magnification = 400×). (**D, E**) Quantitative analysis of the average cross-sectional area of myocytes (CSA) in cardiac tissues and cardiac collagen volume fraction (CVF) in each group. (**F**) The hydroxyproline concentration of the left ventricular tissues. *P< 0.05 vs sham group; #P< 0.05 vs TAC group.

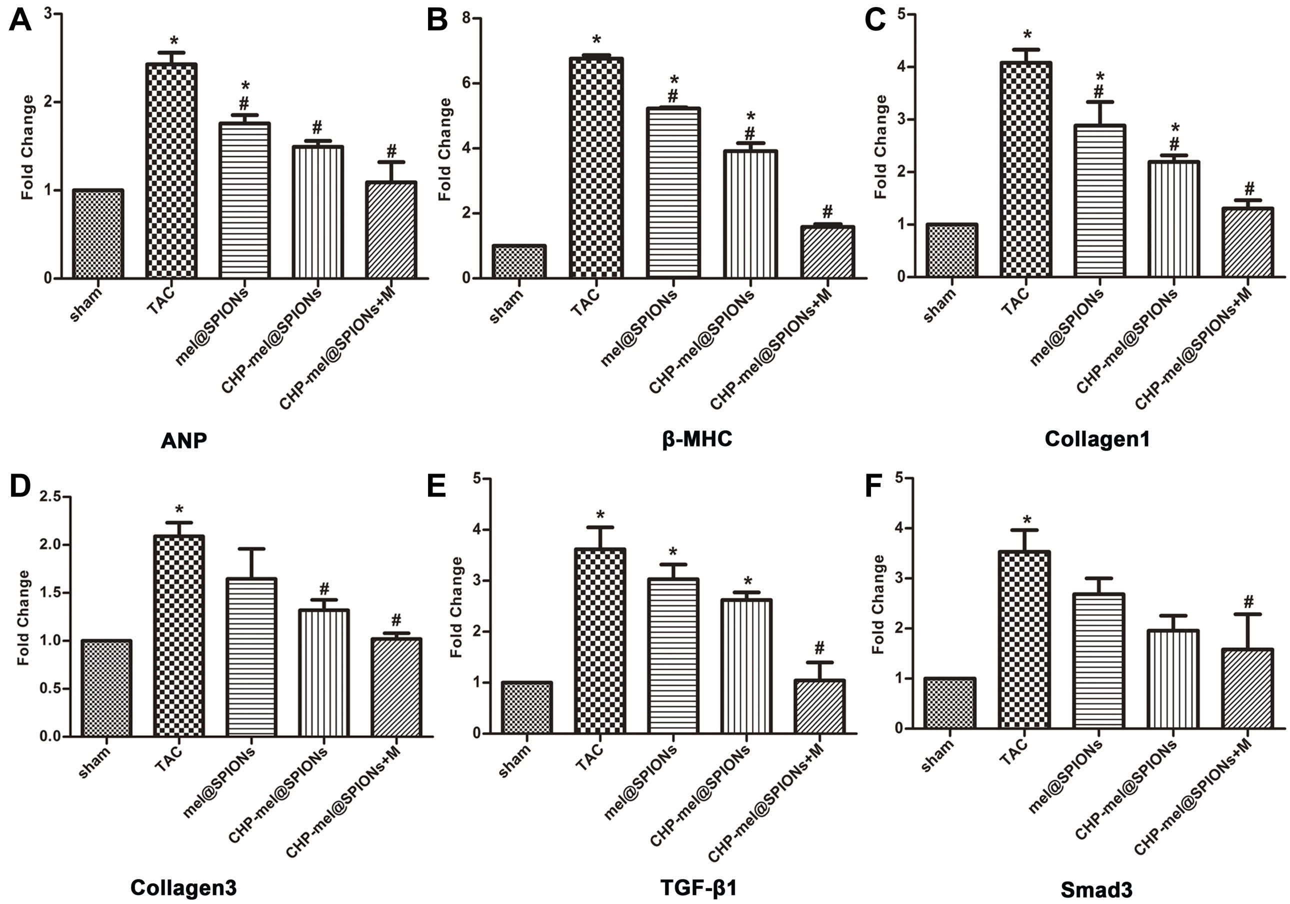

Figure 6 Quantitative RT-PCR analysis of the hypertrophy-related genes and fibrosis markers. (**A**) ANP mRNA level. (**B**) β-MHC mRNA level. (**C**) Collagen 1 mRNA level. (**D**) Collagen 3 mRNA level. (**E**) TGF-β1 mRNA level. (**F**) Smad-3 mRNA level. GAPDH was used as an internal loading control. *P < 0.05 vs sham group; $^{\#}$P < 0.05 vs TAC group.

collagen 1, collagen 3, TGF-β1 and Smad 3 mRNA levels. After treatment, the genes related to cardiac hypertrophy and myocardial fibrosis all exhibited a decreasing trend, indicating that melatonin effectively ameliorated the pressure-induced cardiac hypertrophy and myocardial fibrosis. These results were consistent with previous reports.[16,20,42] The CHP-mel@SPIONs + M group showed a favorable therapeutic as confirmed by the lowest expression of these genes. These datas indicated that melatonin demonstrates anti-fibrotic and anti-hypertrophied properties in TAC-induced cardiac remodeling, which is similar to previous research.[14]

Taken together, these results strongly suggest that by integrating CHP and magnetic targeting, melatonin loading and controlled release properties, the prepared nanoparticles show great potential in facilitating targeted delivery of melatonin for treating cardiac hypertrophy and myocardial fibrosis with high efficacy and low dose. However, the precise mechanism of cardiomyocyte selective binding and internalization of CHP peptide needs to be investigated further. In addition, the associated mechanisms of anti-fibrotic properties of melatonin are not explored in this study, we will design the other experiments for further research. This study promises to provide a solution to the bottleneck in the clinical and experimental translation of targeted therapy of pathological heart conditions in the future.

Conclusion

In this study, a polymeric nanocapsule formulation for a dual-targeting therapeutic system was successfully constructed to deliver melatonin specifically to the heart to ameliorate cardiac hypertrophy and myocardial fibrosis. These CHP-mel@SPIONs were uniform in size and exhibited favorable stability and magnetic properties. In an animal model of cardiac hypertrophy, the targeted delivery provided by the nanoparticles' response to a magnetic field alongside the CHP targeting resulted in an increased uptake of melatonin and functional recovery, evidenced by reduced left cardiac hypertrophy and fibrosis, with a low drug dosage. This design strategy opens up a new approach for the future development of a viable clinical treatment for pressure-induced cardiac hypertrophy.

Acknowledgments

The authors acknowledge the financial support through the Key Science and Technology Innovation Team Project of Shaanxi Province (2014KCT-20), the National Natural Science Foundation of China (81671693), International Cooperation Funding of the China Science and Technology Ministry (2014DFA31980), Shaanxi Provincial Key Project (2017ZDXM-SF-058), and Key R & D Project of Shaanxi Province (2019KW-076).

Disclosure

The authors report no conflicts of interest in this work.

References

1. Chu L, Li P, Song T, et al. Protective effects of tannic acid on pressure overload-induced cardiac hypertrophy and underlying mechanisms in rats. *J Pharm Pharmacol*. 2017;69:1191–1207. doi:10.1111/jphp.2017.69.issue-9
2. Zhao L, Cheng G, Jin R, et al. Deletion of interleukin-6 attenuates pressure overload-induced left ventricular hypertrophy and dysfunction. *Circ Res*. 2016;118:1918–1929. doi:10.1161/CIRCRESAHA.116.308688
3. Shimizu I, Minamino T. Physiological and pathological cardiac hypertrophy. *J Mol Cell Cardiol*. 2016;97:245–262. doi:10.1016/j.yjmcc.2016.06.001
4. Authors/Task Force M, Elliott PM, Anastasakis A, et al. 2014 ESC guidelines on diagnosis and management of hypertrophic cardiomyopathy: the task force for the diagnosis and management of hypertrophic cardiomyopathy of the european society of cardiology (ESC). *Eur Heart J*. 2014;35:2733–2779.
5. Creemers EE, Pinto YM. Molecular mechanisms that control interstitial fibrosis in the pressure-overloaded heart. *Cardiovasc Res*. 2011;89:265–272. doi:10.1093/cvr/cvq308
6. Roche PL, Filomeno KL, Bagchi RA, et al. Intracellular signaling of cardiac fibroblasts. *Compr Physiol*. 2015;5:721–760.
7. Manchester LC, Coto-Montes A, Boga JA, et al. Melatonin: an ancient molecule that makes oxygen metabolically tolerable. *J Pineal Res*. 2015;59:403–419. doi:10.1111/jpi.2015.59.issue-4
8. Yang GH, Li YC, Wang ZQ, et al. Protective effect of melatonin on cigarette smoke-induced restenosis in rat carotid arteries after balloon injury. *J Pineal Res*. 2014;57:451–458. doi:10.1111/jpi.12185
9. Yu L, Fan C, Li Z, et al. Melatonin rescues cardiac thioredoxin system during ischemia-reperfusion injury in acute hyperglycemic state by restoring notch1/hes1/akt signaling in a membrane receptor-dependent manner. *J Pineal Res*. 2017;62.
10. Dominguez-Rodriguez A, Abreu-Gonzalez P, Reiter RJ. The potential usefulness of serum melatonin level to predict heart failure in patients with hypertensive cardiomyopathy. *Int J Cardiol*. 2014;174:415–417. doi:10.1016/j.ijcard.2014.04.044
11. Zhao Y, Xu L, Ding S, et al. Novel protective role of the circadian nuclear receptor retinoic acid-related orphan receptor-alpha in diabetic cardiomyopathy. *J Pineal Res*. 2017;62:e12378.
12. Favero G, Rodella LF, Reiter RJ, et al. Melatonin and its atheroprotective effects: a review. *Mol Cell Endocrinol*. 2014;382:926–937. doi:10.1016/j.mce.2013.11.016
13. Xu L, Su Y, Zhao Y, et al. Melatonin differentially regulates pathological and physiological cardiac hypertrophy: crucial role of circadian nuclear receptor RORalpha signaling. *J Pineal Res*. 2019;67:e12579. doi:10.1111/jpi.12579
14. Zhai M, Liu Z, Zhang B, et al. Melatonin protects against the pathological cardiac hypertrophy induced by transverse aortic constriction through activating PGC-1beta: in vivo and in vitro studies. *J Pineal Res*. 2017;63.
15. Hu W, Ma Z, Jiang S, et al. Melatonin: the dawning of a treatment for fibrosis? *J Pineal Res*. 2016;60:121–131. doi:10.1111/jpi.2016.60.issue-2
16. Yeung HM, Hung MW, Lau CF, et al. Cardioprotective effects of melatonin against myocardial injuries induced by chronic intermittent hypoxia in rats. *J Pineal Res*. 2015;58:12–25. doi:10.1111/jpi.12190
17. Wu Y, Si F, Luo L, et al. The effect of melatonin on cardio fibrosis in juvenile rats with pressure overload and deregulation of hdacs. *Korean J Physiol Pharmacol*. 2018;22:607–616. doi:10.4196/kjpp.2018.22.6.607
18. Jyothirmayi GN, Soni BJ, Masurekar M, et al. Effects of metformin on collagen glycation and diastolic dysfunction in diabetic myocardium. *J Cardiovasc Pharmacol Ther*. 1998;3:319–326. doi:10.1177/107424849800300407
19. Xiao H, Ma X, Feng W, et al. Metformin attenuates cardiac fibrosis by inhibiting the tgfbeta1-smad3 signalling pathway. *Cardiovasc Res*. 2010;87:504–513. doi:10.1093/cvr/cvq066
20. Simko F, Pechanova O, Pelouch V, et al. Effect of melatonin, captopril, spironolactone and simvastatin on blood pressure and left ventricular remodelling in spontaneously hypertensive rats. *J Hypertension Suppl*. 2009;27:S5–10. doi:10.1097/01.hjh.0000358830.95439.e8
21. Karimfar MH, Rostami S, Haghani K, et al. Melatonin alleviates bleomycin-induced pulmonary fibrosis in mice. *J Biol Regul Homeost Agents*. 2015;29:327–334.
22. Harpsoe NG, Andersen LP, Gogenur I, et al. Clinical pharmacokinetics of melatonin: a systematic review. *Eur J Clin Pharmacol*. 2015;71:901–909. doi:10.1007/s00228-015-1873-4
23. Massella D, Leone F, Peila R, et al. Functionalization of cotton fabrics with polycaprolactone nanoparticles for transdermal release of melatonin. *J Funct Biomater*. 2017;9:1.
24. Aeschbach D, Lockyer BJ, Dijk DJ, et al. Use of transdermal melatonin delivery to improve sleep maintenance during daytime. *Clin Pharmacol Ther*. 2009;86:378–382. doi:10.1038/clpt.2009.109
25. Chen J, Yang J, Liu R, et al. Dual-targeting theranostic system with mimicking apoptosis to promote myocardial infarction repair via modulation of macrophages. *Theranostics*. 2017;7:4149–4167. doi:10.7150/thno.21040
26. Bai J, Wang JT, Rubio N, et al. Triple-modal imaging of magnetically-targeted nanocapsules in solid tumours in vivo. *Theranostics*. 2016;6:342–356. doi:10.7150/thno.11918
27. Won YW, McGinn AN, Lee M, et al. Targeted gene delivery to ischemic myocardium by homing peptide-guided polymeric carrier. *Mol Pharm*. 2013;10:378–385. doi:10.1021/mp300500y
28. Vandergriff A, Huang K, Shen D, et al. Targeting regenerative exosomes to myocardial infarction using cardiac homing peptide. *Theranostics*. 2018;8:1869–1878. doi:10.7150/thno.20524
29. Wang X, Chen Y, Zhao Z, et al. Engineered exosomes with ischemic myocardium-targeting peptide for targeted therapy in myocardial infarction. *J Am Heart Assoc*. 2018;7:e008737. doi:10.1161/JAHA.118.008737
30. Eskerud I, Gerdts E, Larsen TH, et al. Left ventricular hypertrophy contributes to myocardial ischemia in non-obstructive coronary artery disease (the MicroCAD study). *Int J Cardiol*. 2019;286:1–6. doi:10.1016/j.ijcard.2019.03.059

31. Sun Y, Zheng Y, Ran H, et al. Superparamagnetic PLGA-iron oxide microcapsules for dual-modality US/MR imaging and high intensity focused US breast cancer ablation. *Biomaterials*. 2012;33:5854–5864. doi:10.1016/j.biomaterials.2012.04.062
32. Ruppert M, Bodi B, Korkmaz-Icoz S, et al. Myofilament ca(2+) sensitivity correlates with left ventricular contractility during the progression of pressure overload-induced left ventricular myocardial hypertrophy in rats. *J Mol Cell Cardiol*. 2019;129:208–218. doi:10.1016/j.yjmcc.2019.02.017
33. Fischer AH, Jacobson KA, Rose J, et al. Cryosectioning tissues. *CSH Protoc*. 2008;2008:pdb.prot4991. doi:10.1101/pdb.prot4939
34. Traynham CJ, Cannavo A, Zhou Y, et al. Differential role of g protein-coupled receptor kinase 5 in physiological versus pathological cardiac hypertrophy. *Circ Res*. 2015;117:1001–1012. doi:10.1161/CIRCRESAHA.115.306961
35. Gao E, Lei YH, Shang X, et al. A novel and efficient model of coronary artery ligation and myocardial infarction in the mouse. *Circ Res*. 2010;107:1445–1453. doi:10.1161/CIRCRESAHA.110.223925
36. Reddy GK, Enwemeka CS. A simplified method for the analysis of hydroxyproline in biological tissues. *Clin Biochem*. 1996;29:225–229. doi:10.1016/0009-9120(96)00003-6
37. El-Gogary RI, Rubio N, Wang JT, et al. Polyethylene glycol conjugated polymeric nanocapsules for targeted delivery of quercetin to folate-expressing cancer cells in vitro and in vivo. *ACS Nano*. 2014;8:1384–1401. doi:10.1021/nn405155b
38. Chen J, Ding J, Wang Y, et al. Sequentially responsive shell-stacked nanoparticles for deep penetration into solid tumors. *Adv Mater*. 2017;29:1701170.
39. Alves NM, Pashkuleva I, Reis RL, et al. Controlling cell behavior through the design of polymer surfaces. *Small*. 2010;6:2208–2220. doi:10.1002/smll.201000233
40. Totaro KA, Liao X, Bhattacharya K, et al. Systematic investigation of EDC/sNHS-mediated bioconjugation reactions for carboxylated peptide substrates. *Bioconjug Chem*. 2016;27:994–1004. doi:10.1021/acs.bioconjchem.6b00043
41. Moens AL, Takimoto E, Tocchetti CG, et al. Reversal of cardiac hypertrophy and fibrosis from pressure overload by tetrahydrobiopterin: efficacy of recoupling nitric oxide synthase as a therapeutic strategy. *Circulation*. 2008;117:2626–2636. doi:10.1161/CIRCULATIONAHA.107.737031
42. Xie YF, Zhang JC, Liu SJ, et al. Effect of melatonin on proliferation and apoptosis of fibroblasts in human hypertrophic scar. *Zhonghua Shao Shang Za Zhi*. 2011;27:422–426.